GEOLOGY | THE GEOLOGICAL SOCIETY OF AMERICA®

https://doi.org/10.1130/G46485.1

Manuscript received 12 April 2019
Revised manuscript received 17 August 2019
Manuscript accepted 22 August 2019

Progressive tilting of salt-bearing continental margins controls thin-skinned deformation

Zhiyuan Ge[1], Michael Warsitzka[2,3], Matthias Rosenau[3] and Rob L. Gawthorpe[1]
[1]Department of Earth Science, University of Bergen, Allégaten 41, 5007 Bergen, Norway
[2]Institute of Geophysics of the Czech Academy of Sciences, Boční II/1401, 141 31 Prague 4, Czech Republic
[3]Helmholtz Centre Potsdam–GFZ German Research Centre for Geosciences, 14473 Potsdam, Germany

ABSTRACT

As a primary driving force, margin tilting is crucial for gravity-driven thin-skinned salt tectonics. We investigated how instant versus progressive margin tilting mechanisms influence salt tectonics using an analogue modeling setup where tilting rate could be controlled. Instant tilting resulted in initially high deformation rates, triggering widely distributed upslope extension and downslope contraction. Later, both the extensional and contractional domains migrated upslope as early extensional structures were successively deactivated, while deformation rates decreased exponentially. In contrast, progressive tilting led to downslope migration of the extensional domain by sequentially formed, long-lived normal faults. Contraction localized on a few, long-lived thrusts before migrating upslope. We attribute the distinct structural evolution of thin-skinned deformation, especially in the extensional domain, in the two tilting scenarios mainly to mechanical coupling between the brittle overburden and underlying viscous material. The coupling effect in turn is largely controlled by the deformation rate. By demonstrating the spatiotemporal variations of structural style and kinematic evolution associated with instant versus progressive tilting, we suggest that such variation is identifiable in nature and therefore can provide a new way to analyze margin tilting histories.

INTRODUCTION

Gravity-driven thin-skinned salt tectonic activity is typically characterized by linked upslope extension and downslope contraction (e.g., Brun and Fort, 2011; Rowan et al., 2004), which significantly affect the tectonostratigraphic evolution of salt-bearing passive margins (e.g., the South Atlantic margins; Marton et al., 2000; Mohriak et al., 2008) and intracratonic rift basins (e.g., the Central Graben, North Sea; Karlo et al., 2014). Sediment loading and margin tilting associated with thermal subsidence and tectonic activity are two major controls of gravity-driven salt tectonics (e.g., Brun and Fort, 2011; Rowan et al., 2004). In nature, margin tilting associated with subsidence is a continuous and protracted process lasting for tens of million years (Fig. 1). Up to now, analogue and numerical models commonly applied an instantaneous, static tilting as the boundary condition, despite its lack of appropriate geological meaning (e.g., Dooley et al., 2007, 2018; Fort et al., 2004; Gaullier et al., 1993; Ings et al., 2004; Mauduit et al., 1997). Although some studies have highlighted the impact of the amount of tilting (Adam et al., 2012; Brun and Fort, 2011; Fort et al., 2004; Ings et al., 2004; Mauduit et al., 1997) and a few have investigated the effect of stepwise (incremental) tilting (Adam et al., 2012; Brun and Fort, 2018; Quirk et al., 2012) upon the structural evolution, there are no modeling studies of thin-skinned salt tectonics where the margin tilting is simulated progressively. As a viscous material, the strength of salt scales proportionally to strain rate, which in turn is mainly controlled by gravitational force during margin tilting, although some other factors may also come into play (e.g., salt thickness; e.g., Dooley et al., 2018; Fort et al., 2004; Weijermars et al., 1993; Zwaan et al., 2016). In simplified terms, salt is expected to be relatively weak during progressive tilting with slowly growing gravitational force, and relatively strong during instant tilting with initially strong gravitational force. Such different tilting scenarios thus may lead to weak versus strong coupling, respectively, between cover sediments and underlying salt. Brittle-viscous coupling plays a key role in distributing strain in lithospheric-scale deformation (e.g., Schueller et al., 2005), as strong and weak coupling effects have been attributed to control wide and narrow rifts, respectively (e.g., Brun, 1999). However, such a coupling effect associated with margin tilting is poorly understood for thin-skinned salt tectonic deformation. Here, we studied the effect of instant versus progressive margin tilting on salt-tectonic structural style and evolution in scaled analogue experiments and compared them to natural salt-influenced margins. In order to mimic natural salt basins, we used a generic basin geometry with a double-wedge shape (Brun and Fort, 2011), such that the salt thickness varied downslope, and included a hinge zone between the two wedges, which typically controls the downslope change from extension to compression (Fig. 2; e.g., Dooley et al., 2018).

MODEL SETUP

The analogue model setup was similar to previous studies where granular materials and polydimethylsiloxane (PDMS) silicone oil were used to simulate brittle sedimentary cover and viscous salt, respectively (e.g., Adam et al., 2012; Fort et al., 2004; Withjack and Callaway, 2000). We used a mixture of quartz sand and foam glass spheres as the cover material to achieve a reasonable density ratio of 1.16 between brittle and viscous layers. The silicone used in this study (KORASILON G30 M) behaves like a Newtonian fluid up to a strain rate of ~10^{-2} s^{-1}, which is well beyond our experimental range (Rudolf et al., 2016). The brittle behavior of the granular mixture used here (Warsitzka et al., 2019) is similar to natural rocks (e.g., Byerlee, 1978). The geometric scaling factor (1 cm in model = 1 km in nature) and time scaling factor (4 h in the model ≈ 1 m.y. in nature) were derived from common scaling procedures (e.g., Adam and Krezsek, 2012; see Table DR1 in the GSA Data

CITATION: Ge, Z., et al., 2019, Progressive tilting of salt-bearing continental margins controls thin-skinned deformation: Geology, v. 47, p. , https://doi.org/10.1130/G46485.1

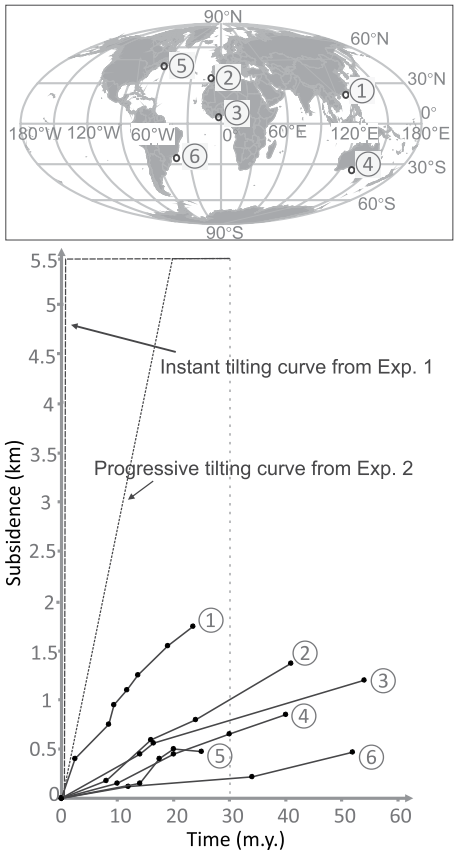

Figure 1. Typical subsidence curves (thermal subsidence–dominated) of modern passive-margin basins and tilting curves applied in this study. Note progressive subsidence curves in all natural cases. 1—South China Sea margin (Lin et al., 2003); 2—Moroccan margin (Le Roy et al., 1998); 3—Côte d'Ivoire–Ghana margin (Clift et al., 1997); 4—Western Australia margin (Falvey and Mutter, 1981); 5—United States Atlantic margin (Swift et al., 1987); 6—Campos Basin, Brazilian margin (Beglinger et al., 2012). Dashed lines are instant and progressive tilting curves (transferred from our experiments based on scaling relationship). Note the gradient of the progressive tilting curve is similar to the highest gradient of natural subsidence curves. Tilting degree of 3.5° is based on Brun and Fort (2011), where a small salt basin needs more tilting to ensure the presence of gravity gliding processes. Furthermore, the value of 3.5° is also comparable to other modeling studies, such as Fort and Brun (2004; 5°), Adam et al. (2012; 3–4°), and Dooley et al. (2018; 3°).

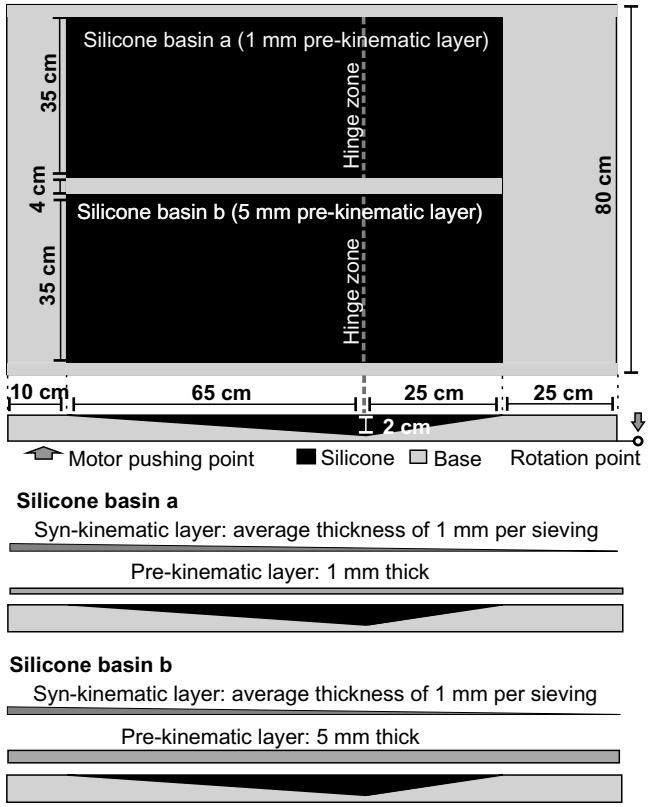

Figure 2. Map view and cross-section view of model design and pattern of sedimentation. Note double-wedge shape of silicone basins and paired basins with different pre-kinematic layer thickness. Also note the motor provides tilting by lifting one side of the model upward. Evolution of basin 'a' in both experiments is documented in the main text; that of basin 'b' serves as a reference and is documented in the Data Repository (see footnote 1). Also note the wedge shape of syn-kinematic sedimentation, reflecting more sediments accumulated near the landward area of a typical passive-margin salt basin.

Repository[1] for details). The base of the experiment was a rigid plate. A basal sand body served as a mold for two identical silicone basins per experiment (Fig. 2). The resultant silicone wedge was thickest at 2 cm in the hinge zone and pinched out gradually toward the basin margins (Fig. 2). The tilting of the basal plate was driven by a computer-controlled motor that started after sieving of a pre-kinematic layer over the silicone basins.

We present two experiments, representing quasi-instant and progressive tilting scenarios, in which a final slope of 3.5° was established in 3.5 min (experiment 1) and at 1°/d (experiment 2), respectively (Fig. 3A). For both experiments, we investigated deformation of two suprasalt, pre-kinematic cover layers with a thickness of 1 mm and 5 mm, respectively. The experiments were run for 5 d with 1 mm (on average) of cover material sieved every 12 h to simulate synkinematic sedimentation (Fig. 2). The models were later sliced to provide cross-sectional views of the final structural styles. During the experiment, the surface of the model was monitored by two charge-coupled device (CCD) cameras, allowing digital image correlation (DIC) for three-dimensional surface analysis at high precision (<0.1 mm) and resolution (e.g., Adam et al., 2005). In the following section, we use downslope surface velocities (V_x), longitudinal surface strain (ε_{xx}), and surface strain rates ($d\varepsilon_{xx}/dt$, 1 h averages) to present experiment results for a pre-kinematic cover thickness of 1 mm (Figs. 3 and 4). The experiments for a thicker pre-kinematic cover (5 mm) gave a similar pattern of structural evolution and so are not described in detail (see Figs. DR1 and DR2). Experimental data were published in Ge et al. (2019).

INSTANT MARGIN TILTING

Instant tilting of 3.5° (experiment 1; Fig. 3A) triggered early basinwide thin-skinned deformation consisting of upslope extension and downslope contraction at high strain rates (3–4 mm/h), which decayed exponentially as the system approached gravitational stability (Fig. 3A). In the initial stage of the experiment, the width of the extensional domain covered ~65% of the basin, bounding the hinge zone (50–60 cm wide; Figs. 3B and 4A). After 37 h, extension retreated to the upper 40% of the basin (Fig. 3B) and further reduced to ~20% toward the end of the experiment (Fig. 3B). Narrowing of the extensional domain occurred by successive upslope deactivation of normal faults (Fig. 4A). After 72 h, the extensional faults near the upslope edge also became inactive due to the depletion of silicone and subsequent welding (Fig. 4A). Early stage contraction was also widely distributed, occupying ~35% of the basin, mainly to the downslope side of the hinge zone (Fig. 3B). The contraction gradually localized onto three main folds and thrusts and migrated upslope in the first 24 h (Fig. 4A), and eventually occupied over 50% of the basin after 72 h (Figs. 3B and 4A). The cross section shows the small extensional structures, which were initially active and widely distributed and then became sequentially inactive and buried at a later stage, when continued extension only occurred near the upslope edge (Fig. 4A). Models with increased pre-kinematic cover thickness (to 5 mm) had a similar structural evolution but smaller

[1]GSA Data Repository item 2019389, results of Basin 1b and 2b, Figures DR1 and DR2, and Table DR1 (scaling relationships), is available online at http://www.geosociety.org/datarepository/2019/, or on request from editing@geosociety.org. Data underlying this study are published open access via the Helmholtz Centre Potsdam GFZ Data Services in Ge et al. (2019), http://doi.org/10.5880/GFZ.4.1.2019.006.

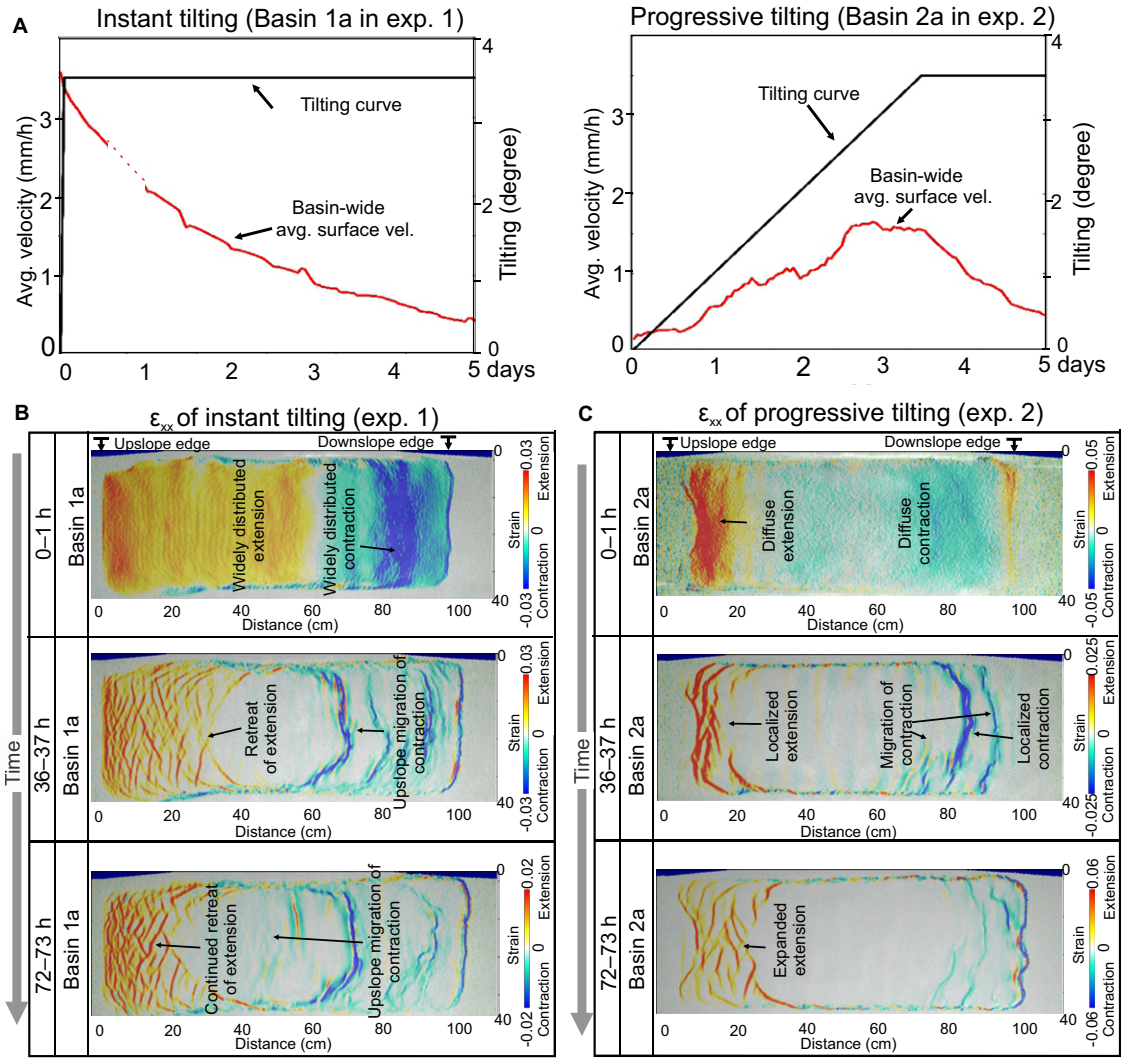

Figure 3. (A) Tilting curve and resulting surface velocity (strain rate) versus time for instant and progressive tilting of basins with a 1 mm pre-kinematic layer. Dashed line of velocity curve is data loss due to a blackout. (B,C) Map views of surface strain for instant tilting (B) and progressive tilting (C) at early (0–1 h), intermediate (36–37 h), and late (72–73 h) stages of basin deformation with 1-mm-thick pre-kinematic cover. Color indicates longitudinal strain (ε_{xx}; warm colors—extension, cold colors—contraction).

extensional and contractional domains, due to the stronger cover (Figs. DR1B and DR2A).

PROGRESSIVE MARGIN TILTING

Progressive tilting (experiment 2; Figs. 3A and 3C) caused basinwide deformation rates to increase slowly, up to 1 mm/h, before decaying exponentially as tilting stopped (Fig. 3A), resulting in different structural evolution compared to instant tilting. Early extension occurred in a narrow zone in the upslope affecting ~10% of the basin area (Figs. 3C and 4B). Instead of retreating upslope, as in the instant margin tilting case, the extensional domain gradually expanded downslope to cover ~30% of the basin area by the end of the experiment (Figs. 3C and 4B). Also in contrast to the instant tilting, the normal faults in the extensional domain mostly stayed active until the end of the experiment with progressive tilting, lacking the deactivation and welding processes observed in the experiment with instant tilting (Fig. 4B). Furthermore, new normal faults (e.g., F1 in Fig. 4B) initiated and grew on the downslope side of the extensional domain, almost 12 h after the formation of the first normal fault (Fig. 3B). In the downslope area, contraction was initially distributed over a wide area, covering over 60% of the basin and encompassing the hinge zone (Fig. 3C). However, after 12 h, when the strain rates increased, the contraction localized on two folds and thrusts, to the downslope side of the hinge zone (Figs. 3A, 3C, and 4B). Minor upslope migration of contraction occurred after 48 h (Fig. 4B). With a thicker pre-kinematic cover (5 mm), the onset of basinwide deformation was significantly delayed (72 h later), and the deformation zones were narrower due to stronger cover, but the overall structural evolution remained similar (see Fig. DR2B).

DISCUSSION

Our experiments suggest that the structural and kinematic evolution of gravity-driven thin-skinned salt tectonics is to a first order controlled by the rate and timing of margin tilting, which dominate other factors like basin geometry, cover, and salt thickness. Instant tilting causes initially high deformation rates and basinwide deformation on multiple, short-lived structures (Fig. 4A). In contrast, progressive tilting triggers lower rates of deformation that localize onto fewer, but longer-lived structures (Fig. 4B). This difference is similar to the brittle-viscous coupling effect that has been recognized in two-layer models of continental rifting experiments (Brun, 1999). For example, Brun (1999) showed that brittle-viscous models subjected to fast extension generate more widely distributed normal faults ("wide rift models") than those subjected to slow extension, where deformation localizes in a single extensional graben ("narrow rift models"). Such variation has been interpreted as due to the strength contrast between the brittle and viscous layers, which is controlled by the strain rate. Specifically, high strain rates lead to a strong viscous layer and strong mechanical coupling between the brittle and viscous layers, while low strain rates result in a weak viscous base flowing laterally and acting as a detachment decoupling the two layers (Brun, 1999).

During the thin-skinned deformation with instant tilting, our salt analogue deformed faster and therefore appeared stronger than the case of progressive tilting. Consequently, strong

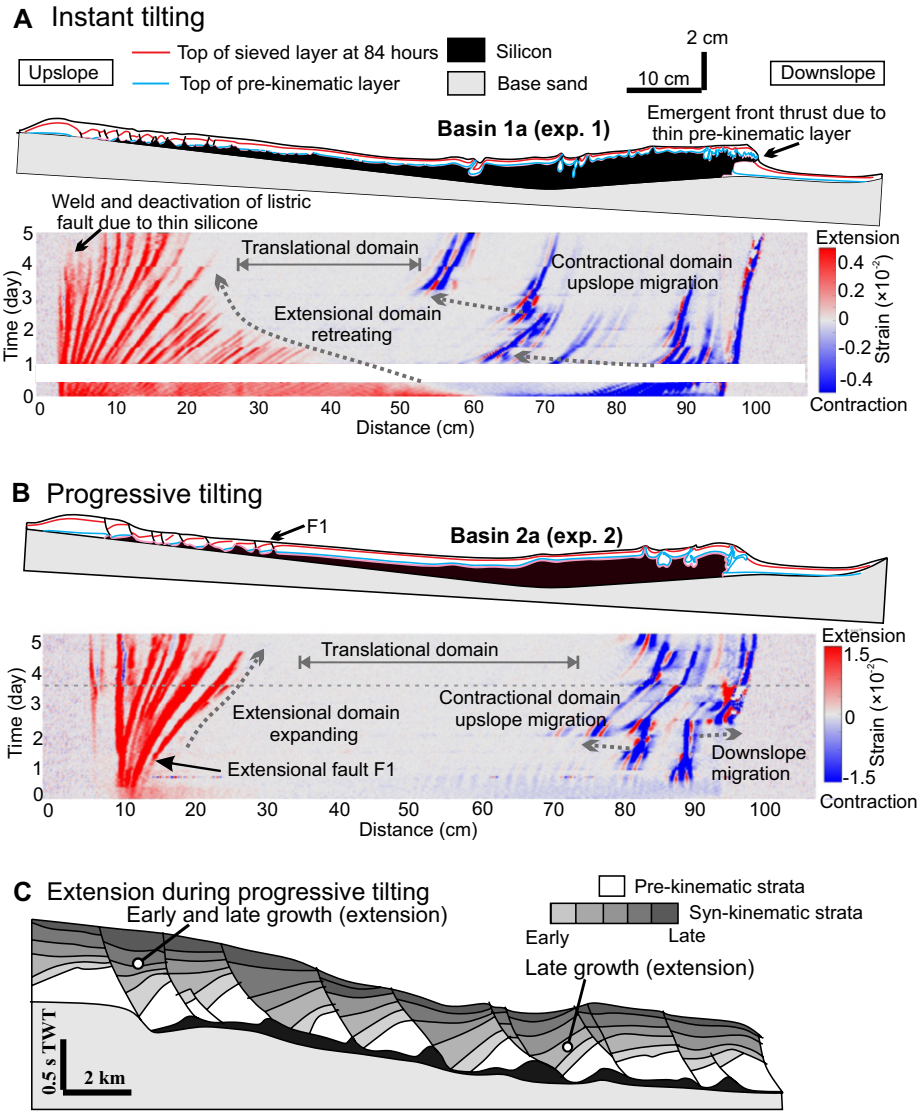

Figure 4. (A) Cross sections and strain rate evolution (1 h increments, red—extension, blue—contraction) of instant tilting in a basin with a 1-mm-thick pre-kinematic layer. Note the upslope retreat of the extensional domain and upslope migration of the contractional domain; 12 h data loss (white band) in strain rate evolution map is due to a blackout. (B) Cross section and strain rate plot (1 h increments) of progressive tilting in a basin with a 1-mm-thick pre-kinematic layer. Note the downslope expansion of the extensional domain. Gray dashed line in strain rate plot indicates the time when tilting stopped. (C) Example of seismic-based section showing sequential occurrence of extensional structures, which indicates progressive tilting. Section is modified from Valle et al. (2001, their figures 6 and 15). TWT—two-way traveltime.

brittle-viscous coupling caused an initially wide area of deformation that became narrower as strain rates decreased (Figs. 3A and 4A). In contrast, during progressive tilting, the salt analogue acted as a weak detachment, allowing the deformation to focus onto a few dominant, long-lived structures as the strain rates gradually increased (Figs. 3A and 4B).

An important observation of progressive tilting is the sequence of faulting. As the extensional domain expands, additional extensional structures form sequentially downslope. For example, in experiment 2, significant extension on fault F1 occurred almost 12 h (3 m.y. in nature prototype) after the formation of the first normal fault (Fig. 4B). Such a sequential deformation style contrasts with the simultaneous occurrence and subsequent deactivation of normal faults observed in instant tilting, which is further complicated by the welding processes that occurred near the upslope edge (Figs. 4A and 4B). Tilting variations have only a limited influence on the contractional domain due to the hinge zone effect (e.g., Dooley et al., 2018). For example, during the initial stage, the hinge zone more effectively delineates the areas of extension and contraction during instant tilting compared to the progressive tilting scenario (Figs. 4A and 4B). Later, in both experiments, the strain is localized onto a few large structures to the downslope side of the hinge zone, before migrating upslope (e.g., Figs. 4A and 4B). The pre-kinematic layer thickness also has a limited impact upon the structural evolution, as a thicker and stronger cover only alters the timing and location of individual structures without changing the deformation style (Fig. DR2).

The variation in extensional faulting sequence can be observed in nature on a semiregional scale of tens of kilometers. As an example, based on a 20-km-long seismic section from the Lower Congo Basin (Valle et al., 2001), we identified an extensional fault in the downslope on which the earliest growth strata are younger than those of the faults in the upslope area (Fig. 4C). Similar examples can also be found in the Campos Basin (Quirk et al., 2012, their figure 4) and the Gulf of Mexico (Curry et al., 2018, their figure 3). We interpret such diachronous growth to indicate the sequential development of extensional structures under progressive margin tilting.

CONCLUSIONS

Using an original analogue modeling approach, we provide the first assessment of the influences of instant versus progressive margin tilting on the structural and kinematic evolution of gravity-driven thin-skinned deformation. Our experimental results suggest that instant margin tilting causes early widespread extension with high strain rates, which then retreat upslope by successive deactivation of normal faults as strain rates decrease. In contrast, progressive margin tilting causes sequential extensional faulting toward the downslope area as strain rates gradually increase. Such variation of extensional styles occurs because the brittle and viscous coupling effect, controlled by strain rates, is initially strong but continuously weakens during instant tilting, whereas it gradually strengthens during progressive tilting. The evolution of the contractional domain is less diagnostic for the mode of tilting and may be more affected by other factors (e.g., basin geometry). The spatiotemporal variation of deformation, especially the sequence of normal faulting, seen in our experiments has implications for subsurface data interpretation and thus may provide a new way to analyze margin tilting. Importantly, this may also help us to identify whether the structures are controlled by gradual thermal subsidence and long-term tectonic activity (progressive tilting) or short-term, more rapid tectonic events (quasi-instant tilting). Finally, we suggest that inclusion of margin tilting scenarios, among many other factors (e.g., salt thickness, basin geometry, etc.), is important for studies of thin-skinned salt tectonics.

ACKNOWLEDGMENTS

We thank E.ON Stipendienfonds (Germany) and the 2018 Trans-national Access (TNA) program of the European Plate Observing System (EPOS) Thematic Core Service Multi-scale Laboratories for funding. Ge thanks Equinor (Norway) for supporting his

postdoctoral fellowship at the University of Bergen. Frank Neumann and Thomas Ziegenhagen are thanked for device construction and technical assistance. Thilo Wrona and Leo Zijerveld are thanked for commenting on an early version of the paper. We thank Tim Dooley, Jürgen Adam, and an anonymous reviewer for their reviews, which improved the quality and clarity of the manuscript. We also thank the editor, Dennis Brown, for editing suggestions.

REFERENCES CITED

Adam, J., and Krezsek, C., 2012, Basin-scale salt tectonic processes of the Laurentian Basin, eastern Canada: Insights from integrated regional 2D seismic interpretation and 4D physical experiments, *in* Alsop, G.I., et al., Salt Tectonics, Sediments, and Prospectivity: Geological Society [London] Special Publications, v. 363, p. 331–360, https://doi.org/10.1144/SP363.15.

Adam, J., Urai, J.L., Wieneke, B., Oncken, O., Pfeiffer, K., Kukowski, N., Lohrmann, J., Hoth, S., van der Zee, W., and Schmatz, J., 2005, Shear localisation and strain distribution during tectonic faulting—New insights from granular-flow experiments and high-resolution optical image correlation techniques: Journal of Structural Geology, v. 27, p. 283–301, https://doi.org/10.1016/j.jsg.2004.08.008.

Adam, J., Ge, Z., and Sanchez, M., 2012, Post-rift salt tectonic evolution and key control factors of the Jequitinhonha deepwater fold belt, central Brazil passive margin: Insights from scaled physical experiments: Marine and Petroleum Geology, v. 37, p. 70–100, https://doi.org/10.1016/j.marpetgeo.2012.06.008.

Beglinger, S.E., van Wees, J.-D., Cloetingh, S., and Doust, H., 2012, Tectonic subsidence history and source-rock maturation in the Campos Basin, Brazil: Petroleum Geoscience, v. 18, p. 153–172, https://doi.org/10.1144/1354-079310-049.

Brun, J.-P., 1999, Narrow rifts versus wide rifts: Inferences for the mechanics of rifting from laboratory experiments: Philosophical Transactions of the Royal Society of London, v. 357, p. 695–712, https://doi.org/10.1098/rsta.1999.0349.

Brun, J.-P., and Fort, X., 2011, Salt tectonics at passive margins: Geology versus models: Marine and Petroleum Geology, v. 28, p. 1123–1145, https://doi.org/10.1016/j.marpetgeo.2011.03.004.

Brun, J.-P., and Fort, X., 2018, Growth of continental shelves at salt margins: Frontiers in Earth Science, v. 6, p. 209, https://doi.org/10.3389/feart.2018.00209.

Byerlee, J., 1978, Friction of rocks, *in* Byerlee, J.D., and Wyss, M., eds., Rock Friction and Earthquake Prediction: Basel, Switzerland, Birkhäuser Basel/Springer, p. 615–626, https://doi.org/10.1007/978-3-0348-7182-2_4.

Clift, P., Lorenzo, J., Carter, A., Hurford, A., and Leg, O., 1997, Transform tectonics and thermal rejuvenation on the Côte d'Ivoire–Ghana margin, west Africa: Journal of the Geological Society [London], v. 154, p. 483–489, https://doi.org/10.1144/gsjgs.154.3.0483.

Curry, M.A.E., Peel, F.J., Hudec, M.R., and Norton, I.O., 2018, Extensional models for the development of passive-margin salt basins, with application to the Gulf of Mexico: Basin Research, v. 30, p. 1180–1199, https://doi.org/10.1111/bre.12299.

Dooley, T.P., Jackson, M.P.A., and Hudec, M.R., 2007, Initiation and growth of salt-based thrust belts on passive margins: Results from physical models: Basin Research, v. 19, p. 165–177, https://doi.org/10.1111/j.1365-2117.2007.00317.x.

Dooley, T.P., Hudec, M.R., Pichel, L.M., and Jackson, M.P.A., 2018, The impact of base-salt relief on salt flow and suprasalt deformation patterns at the autochthonous, parautochthonous and allochthonous level: Insights from physical models, *in* McClay, K.R., and Hammerstein, J.A., eds., Passive Margins: Tectonics, Sedimentation, and Magmatism: Geological Society [London] Special Publications, v. 476, https://doi.org/10.1144/SP476.13.

Falvey, D.A., and Mutter, J.C., 1981, Regional plate tectonics and the evolution of Australia's passive continental margins: BMR Journal of Australian Geology and Geophysics, v. 6, p. 1–29.

Fort, X., Brun, J.-P., and Chauvel, F., 2004, Salt tectonics on the Angolan margin, synsedimentary deformation processes: American Association of Petroleum Geologists Bulletin, v. 88, p. 1523–1544, https://doi.org/10.1306/06010403012.

Gaullier, V., Brun, J.P., Guerin, G., and Lecanu, H., 1993, Raft tectonics: The effects of residual topography below a salt décollement: Tectonophysics, v. 228, p. 363–381, https://doi.org/10.1016/0040-1951(93)90349-O.

Ge, Z., Rosenau, M., Warsitzka, M., and Gawthorpe, R., 2019, Digital Image Correlation Data from Analogue Modeling Experiments Addressing Controls of Tilting Rate on Thin-Skinned Deformation at Salt-Bearing Continental Margins: GFZ Data Services, https://doi.org/10.5880/GFZ.4.1.2019.006.

Ings, S., Beaumont, C., and Gemmer, L., 2004, Numerical modeling of salt tectonics on passive continental margins: Preliminary assessment of the effects of sediment loading, buoyancy, margin tilt, and isostasy, *in* Post, P.J., et al., eds., 24th Annual Gulf Coast Section Society for Sedimentary Geology (SEPM) Foundation Bob F. Perkins Research Conference, December 5–8, 2004, Houston, Texas: Gulf Coast Section, Society for Sedimentary Geology (SEPM), p. 36–68, https://doi.org/10.5724/gcs.04.24.0036.

Karlo, J.F., van Buchem, F.S., Moen, J., and Milroy, K., 2014, Triassic-age salt tectonics of the central North Sea: Interpretation (Tulsa), v. 2, p. SM19–SM28, https://doi.org/10.1190/INT-2014-0032.1.

Le Roy, P., Guillocheau, F., Piqué, A., and Morabet, A., 1998, Subsidence of the Atlantic Moroccan margin during the Mesozoic: Canadian Journal of Earth Sciences, v. 35, p. 476–493, https://doi.org/10.1139/e97-111.

Lin, A.T., Watts, A.B., and Hesselbo, S.P., 2003, Cenozoic stratigraphy and subsidence history of the South China Sea margin in the Taiwan region: Basin Research, v. 15, p. 453–478, https://doi.org/10.1046/j.1365-2117.2003.00215.x.

Marton, G., Tari, G.C., and Lehmann, C.T., 2000, Evolution of the Angolan passive margin, West Africa, with emphasis on post-salt structural styles, *in* Mohriak, W., and Talwani, M., eds., Atlantic Rifts and Continental Margins: American Geophysical Union Geophysical Monograph 115, p. 129–149, https://doi.org/10.1029/GM115p0129.

Mauduit, T., Guerin, G., Brun, J.-P., and Lecanu, H., 1997, Raft tectonics: The effects of basal slope angle and sedimentation rate on progressive extension: Journal of Structural Geology, v. 19, p. 1219–1230, https://doi.org/10.1016/S0191-8141(97)00037-0.

Mohriak, W., Nemcok, M., and Enciso, G., 2008, South Atlantic divergent margin evolution: Rift-border uplift and salt tectonics in the basins of SE Brazil, *in* Pankhurst, R.J., et al., eds., West Gondwana: Pre-Cenozoic Correlations Across the South Atlantic Region: Geological Society [London] Special Publications, v. 294, p. 365–398, https://doi.org/10.1144/SP294.19.

Quirk, D.G., Schødt, N., Lassen, B., Ings, S.J., Hsu, D., Hirsch, K.K., and Von Nicolai, C., 2012, Salt tectonics on passive margins: Examples from Santos, Campos and Kwanza basins, *in* Alsop, G.I., et al., eds., Salt Tectonics, Sediments, and Prospectivity: Geological Society [London] Special Publications, v. 363, p. 207–244, https://doi.org/10.1144/SP363.10.

Rowan, M.G., Peel, F.J., and Vendeville, B.C., 2004, Gravity-driven fold belts on passive margins, *in* McClay, K.R., ed., Thrust Tectonics and Hydrocarbon Systems: American Association of Petroleum Geologists Memoir 82, p. 157–182.

Rudolf, M., Boutelier, D., Rosenau, M., Schreurs, G., and Oncken, O., 2016, Rheological benchmark of silicone oils used for analog modeling of short- and long-term lithospheric deformation: Tectonophysics, v. 684, p. 12–22, https://doi.org/10.1016/j.tecto.2015.11.028.

Schueller, S., Gueydan, F., and Davy, P., 2005, Brittle-ductile coupling: Role of ductile viscosity on brittle fracturing: Geophysical Research Letters, v. 32, L10308, https://doi.org/10.1029/2004GL022272.

Swift, B.A., Sawyer, D.S., Grow, J.A., and Klitgord, K.D., 1987, Subsidence, crustal structure, and thermal evolution of Georges Bank Basin: American Association of Petroleum Geologists Bulletin, v. 71, p. 702–718.

Valle, P.J., Gjelberg, J.G., and Helland-Hansen, W., 2001, Tectonostratigraphic development in the eastern Lower Congo Basin, offshore Angola, West Africa: Marine and Petroleum Geology, v. 18, p. 909–927, https://doi.org/10.1016/S0264-8172(01)00036-8.

Warsitzka, M., Ge, Z., Schönebeck, J.-M., Pohlenz, A., and Kukowski, N., 2019, Ring-Shear Test Data of Foam Glass Beads Used for Analogue Experiments in the Helmholtz Laboratory for Tectonic Modelling (HelTec) at the GFZ German Research Centre for Geosciences in Potsdam and the Institute of Geosciences, Friedrich Schiller University Jena: GeoforschungsZentrum (GFZ) Data Services, http://doi.org/10.5880/GFZ.4.1.2019.002.

Weijermars, R., Jackson, M.P.A., and Vendeville, B., 1993, Rheological and tectonic modeling of salt provinces: Tectonophysics, v. 217, p. 143–174, https://doi.org/10.1016/0040-1951(93)90208-2.

Withjack, M.O., and Callaway, S., 2000, Active normal faulting beneath a salt layer: An experimental study of deformation patterns in the cover sequence: American Association of Petroleum Geologists Bulletin, v. 84, p. 627–651.

Zwaan, F., Schreurs, G., Naliboff, J., and Buiter, S.J.H., 2016, Insights into the effects of oblique extension on continental rift interaction from 3D analogue and numerical models: Tectonophysics, v. 693, p. 239–260, https://doi.org/10.1016/j.tecto.2016.02.036.

Printed in USA